

Structure and Properties of $[(\text{CH}_2\text{OH})_3\text{CNH}_3]\text{H}_2\text{AsO}_4$

A. Waśkowska, S. Dacko^a, and Z. Czapla^a

Institute of Low Temperature and Structure Research Polish Academy of Sciences Okólna 2,
50-422 Wrocław, Poland

^a Institute of Experimental Physics, Wrocław University M. Borna 9, 50-204 Wrocław, Poland

Reprint requests to Prof. Z.C.; E-mail: czapla@ifd.uni.wroc.pl

Z. Naturforsch. **58a**, 722 – 726 (2003); received July 28, 2003

Crystals of $[(\text{CH}_2\text{OH})_3\text{CNH}_3]\text{H}_2\text{AsO}_4$ have been grown, and X-ray diffraction analysis has shown them to be monoclinic, with space group $\text{P}2_1$. A three-dimensional network of hydrogen bonds of the type $\text{O}-\text{H}\cdots\text{O}$ and $\text{N}-\text{H}\cdots\text{O}$ forms strong cation-cation and cation-anion linkages. Stabilizing the structure, they create favourable conditions in the crystal to be polar. The temperature dependent behaviour of the dielectric permittivity, measured along three crystal axes in the range 100–300 K, did not show any evidence for a phase transition, while the pyroelectric properties of the crystal confirmed the lack of a centre of symmetry.

These polar features locate $[(\text{CH}_2\text{OH})_3\text{CNH}_3]\text{H}_2\text{AsO}_4$ among the materials applicable to electrooptics and for the second harmonic generation.

Key words: X-ray Single Crystal Structure; Dielectric and Pyroelectric Properties.

1. Introduction

Tris(hydroxymethyl)aminomethane, $(\text{CH}_2\text{OH})_3\text{CNH}_2$, abbreviated as *Tris*, is commonly known as buffering agent, and its crystalline form at room temperature is noncentrosymmetric, space group $\text{Pn}2_1\text{a}$ [1, 2]. The pseudo-globular *Tris*-molecule forms numerous salts, which being also noncentrosymmetric, are topics of interest due to their potential use in nonlinear optics and signal processing. Besides, the *Tris*-based compounds often show interesting physical properties related to the structural and ferroelectric phase transitions [2–4]. These properties are determined by a strong ability of *Tris* to build a system of hydrogen bonds in the crystal structure. The dynamics of protons, especially their site disorder, is one of the decisive factors determining the ferroelectricity and structural phase transitions.

Recently it was shown that trigonal $(\text{CH}_2\text{OH})_3\text{CNH}_3)_2\text{SiF}_6$, abbreviated as TSF, undergoes a first-order, structural phase transition of a ferroelastic nature, connected with a freezing of reorientational movements of the SiF_6 ions below $T_C = 177$ K [4]. *Tris*(phosphite), $(\text{CH}_2\text{OH})_3\text{CNH}_3]\text{HPO}_3\text{H}$ denoted by TPH is reported to crystallize in the monoclinic system with the space group $\text{P}2_1$ [3]. The polar properties of TPi are related to ordering of protons in hydrogen bonds, which form linear chains of HPO_3^- groups in the structure. In this way, at room temperature the crystals

become polar along the *b*-axis and can be candidates for both the second harmonic generation (SHG) and electrooptics. These effects are widely known in KDP or KTP.

The purpose of the present studies was to grow single crystals of $[(\text{CH}_2\text{OH})_3\text{CNH}_3]\text{H}_2\text{AsO}_4$ – *Tris*(dihydrogen)arsenate (TDA) and describe their symmetry, structure and physical properties in order to characterize their polar features concerning pyroelectric or ferroelectric phenomena.

2. Experimental

The crystals of TDA were grown from water solutions containing stoichiometric quantities of *Tris* and As_2O_5 . The single crystals were obtained by a slow evaporation method at a constant temperature of 303 K.

The X-ray intensity data were obtained with a 4-circle Oxford Diffraction/CCD single crystal diffractometer and graphite monochromated $\text{MoK}\alpha$ radiation ($\lambda = 0.71073$ Å). The data were collected using the ω -scan technique. 9 runs, each including 100 images, were performed at different angular positions ($\Delta\omega = 1.0^\circ$, exposure time 25 s per frame). One image, selected as a standard, was monitored after every 50 images to control the stability of the crystal and of the electronic system. The data were corrected

Table 1. Crystal data, experimental details and structure refinement parameters.

Empirical formula	[(CH ₂ OH) ₃ CNH ₃] ₂ AsO ₄
Formula weight	263.08
Temperature (K)	263
Wavelength (Å)	0.71073
Crystal system, space group	Monoclinic, P2 ₁
Unit cell dimensions (Å)	$a = 8.235(2)$ $b = 6.1820(10)$ $c = 9.861(2)$ $\beta = 104.81(3)^\circ$
Volume (Å ³)	485.33(17)
Z, Calculated density (Mg/m ³)	2, 1.800
Absorption coefficient (mm ⁻¹)	3.512
$F(000)$	268
Crystal size (mm)	$0.30 \times 0.27 \times 0.25$
θ range for data collection	3.73 to 46.24°
Limiting indices	$-13 \leq h \leq 16,$ $-11 \leq k \leq 9,$ $-14 \leq l \leq 19$
Reflections collected / unique	8971 / 5421 [R(int) = 0.022]
Refinement	Full-matrix least-squares on F^2
Data / restraints / parameters	5421 / 1 / 134
Goodness-of-fit on F^2	0.809
Final R indices [$I > 2\sigma(I)$]	$R_1 = 0.0258, wR_2 = 0.0488$
R indices (all data)	$R_1 = 0.0429, wR_2 = 0.0537$
Absolute structure parameter	-0.012(6)
Extinction coefficient	0.109(3)
Largest diff. peak and hole (eÅ ⁻³)	0.737 and -0.783

for Lorentz and polarization effects. Analytical absorption correction was calculated using the face-indexed procedure of *CrysAlis* software [5]. The structure was solved with the heavy atom method, followed by difference Fourier calculations and refined by the full matrix least-squares method on F^2 data (SHELXS97 and SHELXL97 program systems, respectively [6, 7]). Hydrogen atoms were included from geometry and constrained at their positions assuming the ‘ride-on’ model with refined isotropic temperature factors. The final difference Fourier map was essentially featureless, with residual minima and maxima close to the As ion. The refinement showed significant presence of extinction, hence this parameter was also included in the refinement according to the procedure given in [8]. The crystal data and details of the experimental conditions and the refinement parameters are given in Table 1.

The electric permittivity was measured along three perpendicular directions (a , b and $c^* = c \sin \beta$) using a computer controlled HP 4284 A LCR-meter in the frequency range 1 kHz–1 MHz. Polarisation changes in the crystal were observed by means of the pyroelectric method. The electric permittivity and the pyroelectric properties were studied in the temperature range

Table 2. Atomic coordinates ($\text{\AA} \times 10^4$) and equivalent isotropic displacement parameters ($\text{\AA}^2 \times 10^3$). U_{eq} is defined as one third of the trace of the orthogonalized U_{ij} tensor.

	x	y	z	U_{eq}
As(1)	6496(1)	4208(1)	6391(1)	22(1)
O(1)	4405(1)	4206(3)	5781(1)	27(1)
O(2)	7189(2)	4993(2)	8027(1)	32(1)
O(3)	7281(2)	1675(2)	6293(2)	46(1)
O(4)	7363(2)	5709(3)	5296(1)	38(1)
O(12)	2712(2)	3718(2)	7817(1)	32(1)
O(13)	4091(1)	10079(2)	9056(1)	30(1)
O(14)	687(1)	8132(2)	9167(1)	26(1)
N(1)	2549(1)	6606(2)	10034(1)	20(1)
C(1)	1942(2)	7273(2)	8528(1)	19(1)
C(2)	1396(2)	5243(3)	7643(2)	25(1)
C(3)	3396(2)	8392(3)	8109(2)	25(1)
C(4)	455(2)	8826(3)	8395(2)	24(1)

Table 3. Selected bond lengths (Å) and angles (deg).

As(1)-O(2)	1.6412(11)	As(1)-O(1)	1.6727(10)
As(1)-O(3)	1.7061(13)	As(1)-O(4)	1.7114(13)
O(12)-C(2)	1.413(2)	O(13)-C(3)	1.419(2)
O(14)-C(4)	1.419(2)	N(1)-C(1)	1.498(2)
C(1)-C(2)	1.530(2)	C(1)-C(3)	1.529(2)
C(1)-C(4)	1.535(2)		
O(2)-As(1)-O(1)	114.89(6)	O(2)-As(1)-O(3)	106.57(6)
O(1)-As(1)-O(3)	110.41(8)	O(2)-As(1)-O(4)	111.33(7)
O(1)-As(1)-O(4)	109.30(7)	O(3)-As(1)-O(4)	103.71(8)
N(1)-C(1)-C(2)	108.35(12)	N(1)-C(1)-C(3)	107.82(11)
C(2)-C(1)-C(3)	110.68(12)	N(1)-C(1)-C(4)	108.33(11)
C(2)-C(1)-C(4)	110.65(12)	C(3)-C(1)-C(4)	110.90(13)
O(12)-C(2)-C(1)	111.95(12)	O(13)-C(3)-C(1)	111.51(13)
O(14)-C(4)-C(1)	112.84(13)	O(14)-C(4)-H(41)	111.49(14)

100 K–370 K. Hysteresis loops were observed with the Sawyer-Tower circuit at a frequency 50 Hz.

3. Results and Conclusion

Large crystals with a volume of 2–3 cm³ and good quality were easily obtained in a period of 4 weeks.

The crystal structure of TDA with an atom numbering scheme is shown in Figure 1. The atomic positions and their thermal vibration amplitudes (U_{eq}) are given in Table 2. The structure calculations established that the crystal symmetry does not contain a centre of inversion. The positional parameters represent the absolute configuration of the structure, which was determined by comparing the alternative least-squares refinement and the value of the Flack parameter. The formula unit consists of a protonated (CH₂OH)₃CNH₃⁺ cation and a distorted tetrahedral (H₂AsO₄)⁻ group (Table 3). In the crystal structure each hydroxyl group of *Tris* is involved in hydrogen bonding of the type O–H...O

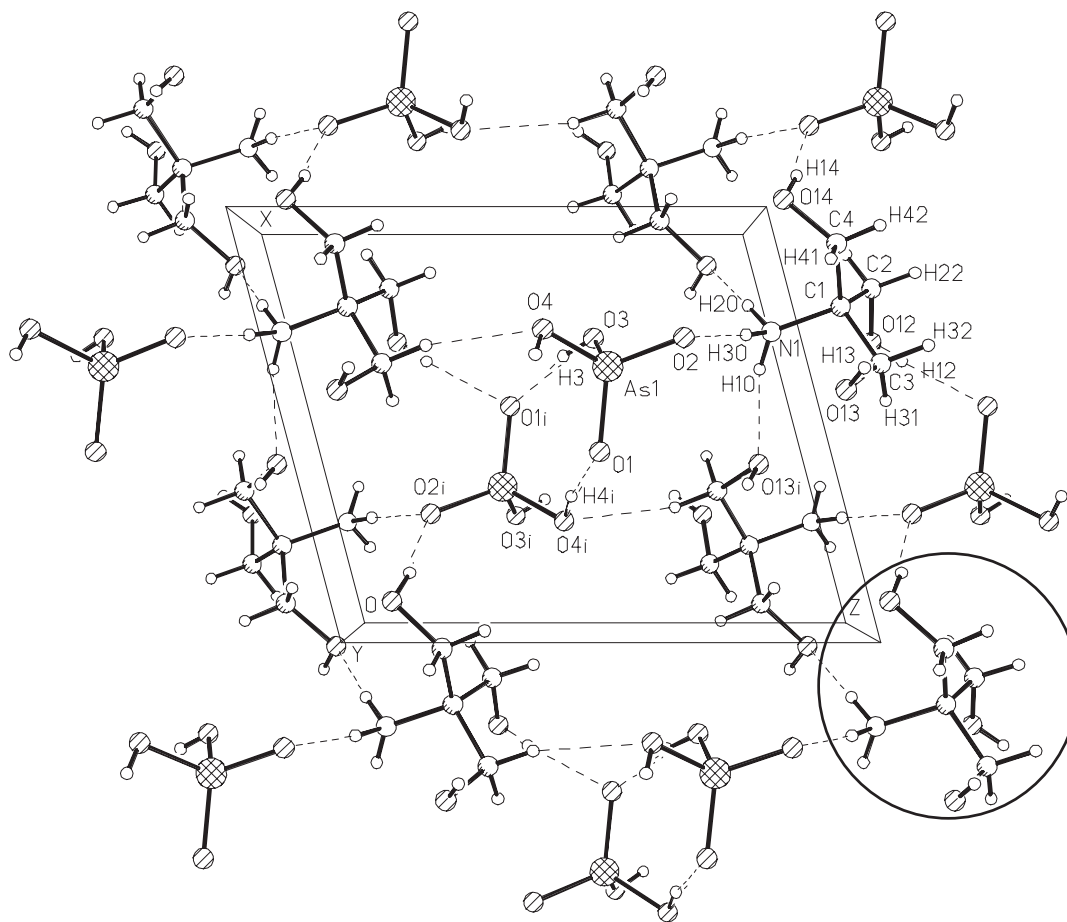


Table 4. Hydrogen bonds in $[(\text{CH}_2\text{OH})_3\text{CNH}_3]\text{H}_2\text{AsO}_4$ (\AA and deg).

Symmetry codes: ⁱ $1-x, 1/2-y, 1-z$; ⁱⁱ $x, 1+y, z$; ⁱⁱⁱ $x-1, y, z$;
^{iv} $1-x, y-1/2, 2-z$; ^v $-x, y-1/2, 2-z$; ^{vi} $1-x, 1/2+y, 2-z$.

and 2.671(3) Å, respectively (Table 4). On the other hand, H10 and H20 of the protonated amino group of *Tris* are involved in strong hydrogen bonds of the type N–H...O, linking O13 and O14 of two symmetrically related *Tris* molecules. In this case O13 and O14 are acting as the electron acceptors. The N–H...O distances are 2.843(3) Å and 2.865(3) Å, respectively, while the typical N–H...O bond length is 2.89 Å [9, 10]. The third proton of *Tris*, H30, makes a connection with O2 of the anionic group. The distance N–H30...O2 is 2.806(3) Å.

The tetrahedral distortion of the AsO₄ group with two elongated As–O distances is a consequence of the presence of another set of hydrogen bonds linking two symmetrically related anionic groups through O3–H3...O1_i and O4_i–H4_i...O1 [2.643(2) and 2.670(2) Å]. Such a network of strong hydrogen bonding, with H-atoms ordered at their sites, stabilizes

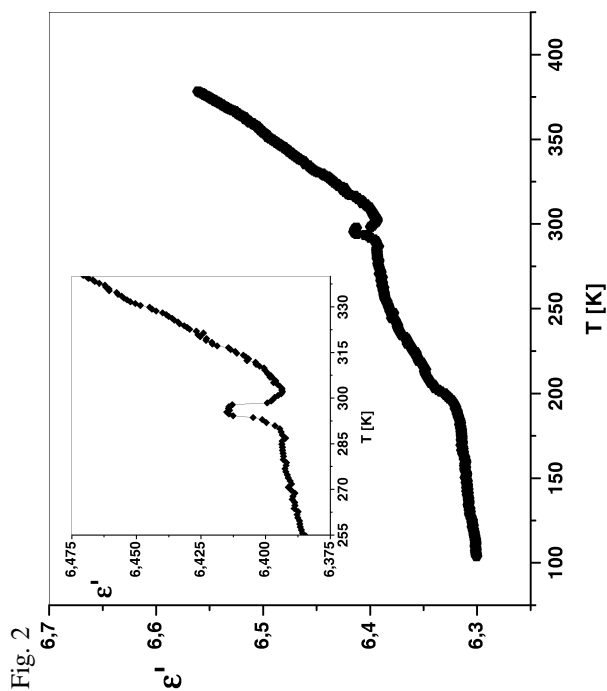


Fig. 2

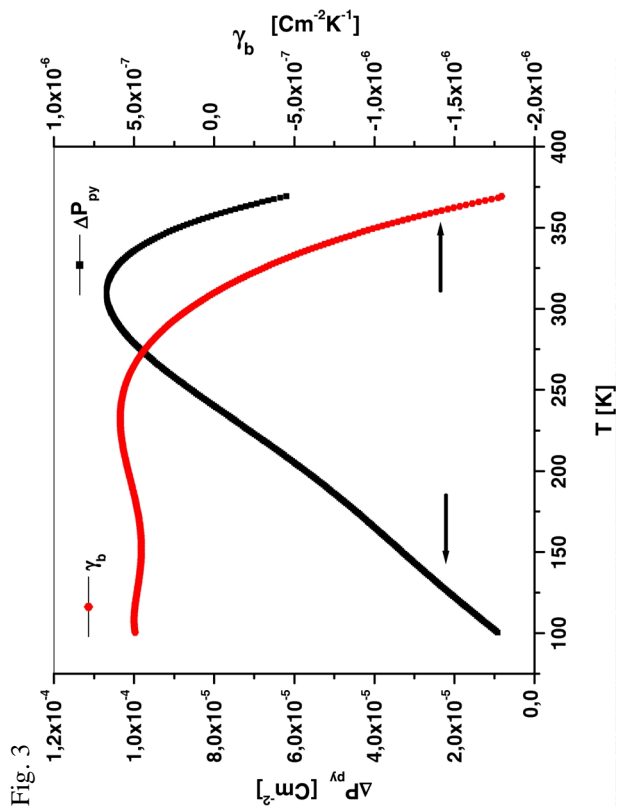


Fig. 3

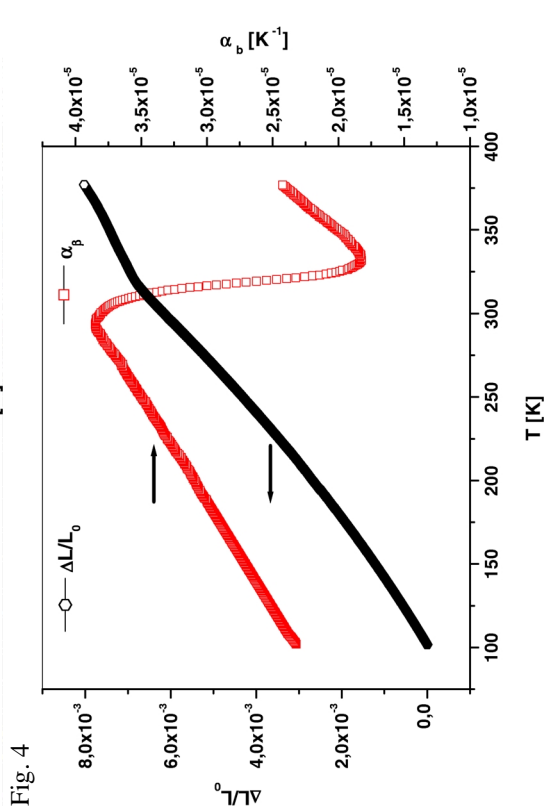


Fig. 4

Fig. 2. Dielectric permittivity along the crystal *b*-axis as a function of temperature.

Fig. 3. Variation of the polarization change (ΔP_y) and of the pyroelectric coefficient (γ_b) along the *b*-axis.

Fig. 4. Dilatation ($\Delta L/L$) and the thermal expansion coefficient (α_b) along the *b*-axis.

the crystal structure and allows expectation of polar properties.

This assumption finds confirmation in the experimental results shown below. The dielectric permittivity, measured in the temperature range 100–350 K along the crystallographic *b*-axis, is shown in Figure 2. A clear change of character of the permittivity takes place in this direction at about 298 K. The temperature dependence of the permittivity along the *a* and *c**-axes does not reveal any anomalous behaviour. The values of the permittivity are rather low, but no anomalies which could suggest a phase transition were observed on cooling. At higher temperatures close to the melting point (450 K) a considerable increase of the conductivity has been observed.

The polar properties of the crystal were checked with the Sawyer-Tower circuit. As no hysteresis loops were present, we came to the conclusion that the crystal is not ferroelectric. The measurements of the pyroelectric properties in the range of 100–320 K showed the electric current evolution in the *b*-direction. This means that the crystals of TDA are polar and pyroelectric. The temperature dependence of the change of spontaneous polarisation ΔP_y and of the pyroelectric coefficient γ_b are shown in Figure 3. A change of direction of the pyroelectric current takes place at about 315 K, manifesting itself as a broad maximum in the temperature dependence of ΔP_y . To investigate this specific behaviour in more detail, the dilatation along the unique *b*-axis was measured in the range 100–380 K (Figure 4). A kind of anomaly, occurring between 290 K and 325 K, has no influence on the pyroelectric properties, in the sense that the maximum in ΔP_y is not directly linked with the dilatation. It can rather be attributed to some modifications in the crystal structure at elevated temperatures. To answer this

question would require systematic structural studies at varying temperature. A similar behaviour of polarization has been observed in $\text{Li}_2\text{SeO}_4 \cdot \text{H}_2\text{O}$ [11, 12] where at 100 K the dipole moment of the unit cell was reversed as a result of temperature dependent rotation of water molecules [13].

In general, the present studies over the temperature range 100–380 K established that the crystal structure of TDA is noncentrosymmetric, and its polar properties enable potential use in nonlinear optics. The anomalies observed in the temperature dependent variation of the dielectric permittivity and dilatation do not exclude a phase transition in a high temperature region.

It should be mentioned that our preliminary studies on *Tris*(dihydrogenphosphate) $[(\text{CH}_2\text{OH})_3\text{CNH}_3]\text{H}_2\text{PO}_4$ with the unit cell parameters $a = 8.213(2)$, $b = 6.188(1)$, $c = 9.611(2)$ Å and $\beta = 106.27(3)$ and monoclinic space group $P2_1$ showed the crystal to be isomorphous with TDA. Provisional observations suggest a strong SHG ability [14]. Thus both of these *Tris*-comprising materials seem to be applicable to second harmonic generation.

To conclude, it can be stated that:

1. X-ray diffraction structure determination proved that $[(\text{CH}_2\text{OH})_3\text{CNH}_3]\text{H}_2\text{AsO}_4$ crystallises in the non-centrosymmetric space group $P2_1$.
2. The polar properties of TDA were confirmed by the measurements of dielectric and pyroelectric effects. The polar axis is directed along the crystal *b*-axis. The maximum in temperature dependent variation of polarization change ΔP_y was observed at about 315 K. The pyroelectric effect is not related to dilatation of the sample.

This work was supported by the University of Wrocław under grant 2016/W/IFD/02.

- [1] D. Eilerman and R. Rudman, *J. Chem. Phys.* **72**, 10 (1980).
- [2] J. Li Tamarit, M. A. Perez-Jubindo, and M. R. de la Fuente *J. Phys.: Condens. Matter* **9**, 5469 (1997).
- [3] M. Th. Averbuch-Pouchot, *C. R. Acad. Sci. Paris* **318**, 191 (1994).
- [4] B. Kosturek, Z. Czapla, and A. Wařkowska, *Z. Naturforsch.* **58a**, 121 (2003).
- [5] Oxford Diffraction 2002, CrysAlis CCD and CrysAlis RED, Oxford Diffraction Ltd.
- [6] G. M. Sheldrick, SHELXS 97, Program for Solution of Crystal Structures, University of Göttingen, Germany 1997.
- [7] G. M. Sheldrick, SHELXL 97, Program System for the Determination and Refinement of Crystal Structures, University of Göttingen, Germany 1997.
- [8] A. C. Larson, *Acta Cryst.* **23**, 664 (1967).
- [9] L. N. Kuleshova and P. M. Zorkii, *Acta Cryst.* **B37**, 1363 (1981).
- [10] T. Steiner and W. Saenger, *Acta Cryst.* **B50**, 348 (1994) and references therein.
- [11] S. B. Lang, *Phys. Rev.* **B4**, 3603 (1971).
- [12] N. D. Gavrilova, E. G. Maksimov, V. K. Novik, and S. N. Drozhdin, *Fiz. Tverd. Tela* **27**, 2597 (1985).
- [13] K. M. Karpinen, R. Liminga, Å. Kvick, and S. C. Abrahams, *J. Chem. Phys.* **80**, 351 (1988).
- [14] R. Klein, private information (2003).